

## THERMAL BEHAVIOUR OF MODIFIED FAUJASITES\*

A. J. CHANDWADKAR and S. B. KULKARNI

*National Chemical Laboratory, Pune 411004, India*

(Received December 13, 1979)

A derivatograph was used to follow the modification of the skeleton structure and thermal stability of zeolites in sodium and ammonium forms. Analogous investigations were carried out by independent methods such as IR and X-ray. Comparison showed good agreement between the results. The controlled dealumination of the Y-type zeolite enhanced the thermal stability.

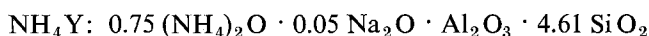
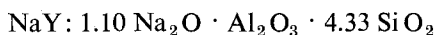
Modified zeolites prepared by treatment with ethylene diamine tetraacetic acid ( $H_4$  EDTA) and subsequent activation profoundly alter their structures. Samples treated in this manner show differences in both catalytic activity and adsorptional properties, depending on the  $SiO_2/Al_2O_3$  ratio. In particular, the crystallinity of the Y-type zeolite is maintained up to the elimination of roughly one-half of the aluminium [1], and then it begins to fall off while the catalytic activity in cracking reactions rises [2]. The zeolite-based catalysts containing protons and polyvalent cations are more active [3] as compared to alkali metal zeolites.

As regards the cation-deficient zeolites, the thermal behaviour of Y-type zeolites exchanged with ammonium ions has been reported [4,5] to some extent. The effects of the variation of the silica-alumina ratio and the bed geometry on the dehydroxylation and thermal stability of the products have been studied [4] and related [5] to the residual  $Na^+$  ions in the Y-type zeolite. Kerr [4, 6] proposed that ultra-stabilization involved the removal of framework aluminum, which is held as  $Al(OH)_2^+$ ,  $Al(OH)^{2+}$  or  $Al^{3+}$  ions. The present study was undertaken to obtain additional evidence on the thermal stability of dealuminated zeolites by thermal, X-ray and IR.

### Experimental

Binder-free Y-type zeolites in the sodium (SK-40) and ammonium (SK-41) forms were obtained from Union Carbide (USA), dried at  $120^\circ$  and kept for about a week over a saturated solution of ammonium chloride at room temperature. The chemical compositions of the dehydrated zeolites, determined by gravimetric analysis, were as follows:

\* NCL Communication No. 2373. Presented in part at the First National Symposium on Thermal Analysis at I.I.T. Madras, 1978.



The dealuminated NaY- $\alpha$  and NH<sub>4</sub>Y- $\alpha$  zeolites (where  $\alpha$  signifies the percentage dealumination) were obtained [6–8] by chelation with H<sub>4</sub>EDTA. The decationated (HY- $\alpha$ ) zeolites were prepared from NH<sub>4</sub>Y by controlled heat treatment at 500°.

Simultaneous thermogravimetry and differential thermal analysis curves were obtained using the derivatograph (MOM-Budapest, Hungary, type OD-102) [9]. Samples weighing 400 mg were run in air atmosphere with a constant heating rate of 10°/min and a maximum temperature of 1200° using a Pt/Rh thermocouple. Precalcined Al<sub>2</sub>O<sub>3</sub> was used as standard. X-ray powder diffraction patterns of hydrated zeolite powder (240 mesh) were recorded on a Philips X-ray diffractometer, model PW-1060/00, with a stripchart recorder (speed 10 mm/min) and pulse height analyzer, using copper K $\alpha$  radiation ( $\lambda = 1.5405 \text{ \AA}$ ).

Infrared spectra were recorded in the frequency range 250 to 1300 cm<sup>-1</sup>, using a Perkin Elmer-221 spectrometer. Nujol mulls or KBr pellets of the hydrated samples were used to record the spectra.

### Results and discussion

The NaY TG curve records a continuous weight loss up to 700°, which amounts to 29.8% (Fig. 1). A typical large weight loss step (50–350°) and a small step (520–620°) indicates two-stage water desorption, mainly due to dehydration and dehydroxylation, respectively.

Differential thermal analysis provides an excellent method of separating and identifying individual step. The differential thermal curve of zeolite is characterized by a sharp and strong endothermic peak (50–350°) and a small exothermic peak around 900°. The low-temperature endotherm is due to loss of water from the zeolite cavity, while the exotherm is due to structural change to the amorphous form or mullatization [10]. The thermal data on the modified NaY- $\alpha$  zeolites are analyzed in Table 1. The DTA and DTG peak maxima ( $T_{\text{max}}$ ) for NaY zeolite

Table 1  
Thermal analysis results

Zeolite	DTA peak		DTG peak		Exotherm, $T_{\text{max.}}$ , °C	$E$ kJ/mol
	$T_{\text{max.}}$ , °C	Base width, °C	$T_{\text{max.}}$ , °C	Base width, °C		
NaY	224	54–441	199	42–355	900	25.5
NaY-12.9	210	35–316	180	35–330	903	24.7
NaY-23.5	205	49–336	178	49–326	940	23.4
NaY-40.2	163	39–267	163	39–299	946	22.2
NaY-56.5	143	51–242	132	40–210	998	18.0

occur at 224 and 199°, showing the maximum rate of dehydration at this temperature. The value of  $T_{\max}$  continuously decreases with progressive Al extraction from the zeolite framework.

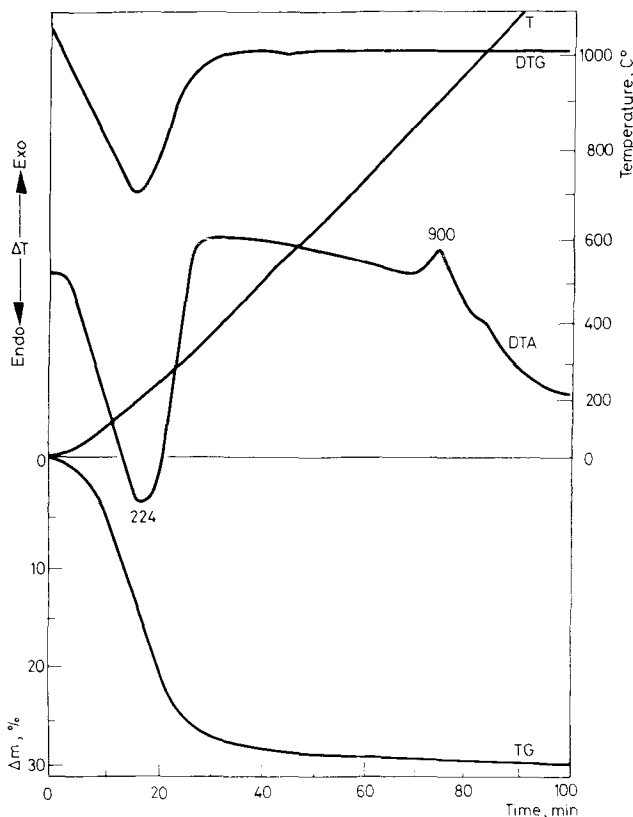


Fig. 1. TG, DTG and DTA curves of NaY zeolites

The progress of dealumination is expressed as:  $x \text{H}_4\text{EDTA} + \text{NaAlO}_2(\text{SiO}_2)_y \rightarrow x \text{NaAlEDTA} \cdot \text{H}_2\text{O} + (\text{NaAlO}_2)_{1-x}(\text{SiO}_2)_y + \text{H}_2\text{O}$  where  $x \leq 1$  and  $y \geq 2.5$  shows that for each atom of Al extracted, one  $\text{Na}^+$  ion is removed from the zeolite. Thus, with the reduction in the number of Na ions, dehydration of the zeolite becomes faster and occurs at lower temperature. This effect in turn is related to the greater strength of the bonds between the water and  $\text{Na}^+$  cations [11]. This is confirmed by a steady decrease in the adsorption heats with increase in the degree of decationization and dealumination [12]. The increase in the exothermic peak temperature from 900 to 998° for dealuminated Y-type zeolites is indicative of higher thermal stability for the Al-deficient samples.

The TG curves for dealuminated and decationated  $\text{NH}_4\text{Y}$  zeolites distinctly show two-step weight loss. For the  $\text{NH}_4\text{Y}$  sample the first step is attributed [13] to the liberation of water and ammonia, and the second step to the loss of structural water; these merge into one step on further modification.

DTA curves (Fig. 2) of  $\text{NH}_4\text{Y}-\alpha$  show four distinct peaks. Decomposition of ammonia is represented as follows:



The heat change should be endothermic on the basis of bond energy considerations and the DTA curves confirm this point. The first endothermic peak for  $\text{NH}_4\text{Y}$  at  $202^\circ$  is responsible for the desorption of physically sorbed water and partly chemisorbed water. The second stage endotherm around  $290^\circ$  is due to the dissociation of  $\text{NH}_3$  from  $\text{NH}_4^+$  ions in the small pore systems, and the third endotherm ( $250-436^\circ$ ) is due to the dissociation of  $\text{NH}_4^+$  in the large pore system. The fourth endotherm ( $550^\circ$ ) is due to dehydroxylation [14] and is related to the crystallographic site occupancy described by Smith [15]. The data thus show that physically sorbed water, ammonia and water of constitution are evolved in successive stages, though such stages are not always clearly separable. In the case of each zeolite, ammonia evolution begins before all the physically sorbed water is removed. It is concluded that the ammonium ion has been completely decomposed to ammonia and residual hydrogen ions at the temperature immediately above that at which ammonia is last detected ( $500^\circ$ ).

Endotherms of decationated ( $\text{HY}-\alpha$ ) zeolites are sharp and narrow as compared to those of  $\text{NH}_4\text{Y}-\alpha$ , and their width goes on decreasing as one proceeds towards a higher dealuminated sample. On comparing the exotherms of  $\text{NH}_4\text{Y}$  and  $\text{HY}$  zeolites, it is observed that the exotherm associated with ammonia removal was absent for  $\text{HY}$  (around  $500^\circ$ ), which was finally confirmed by microanalysis and gravimetric analysis. These observations agree with an earlier report [16]. Exothermic peaks ( $900-990^\circ$ ) and temperature of mullatization in the range  $1030-1065^\circ$  are attributed to structural transformation, as confirmed by the X-ray analysis [17].

The exotherms for the deep-bed and shallow-bed calcined samples prepared under similar conditions occur at  $1040$  and  $900^\circ$ , respectively. The order of thermal stability is  $\text{HY} (\text{DB-6}) > \text{HY} (\text{SB-6})$ , where DB-6 and SB-6 means deep-bed and shallow-bed calcination for 6 hours. From the studies on the nature of deep-bed calcined ammonium zeolite, Y and Al-deficient zeolite, it was concluded that the stability of the ultrastable faujasite was imparted [18] only by cationic Al and that an Al-deficiency in itself did not contribute to stability.

In order to find the physical significance of the process of desorption, it is assumed that the numerical value of the order of reaction ( $n$ ) is proportional to the number of monomolecular layers that constitute the adsorption film of water on the surface of the zeolite, and the activation energy ( $E$ ) is related to the energy of desorption. The value of  $E$  was calculated from TG curves using the Coates-Redfern equation (1) [19] and the Piloyan-Novikova equation (2) [20]. Similarly,

$E$  from DTA curves was also calculated from relation (3) described by Piloyan and Novikova [20]. The order of reaction was calculated independently from the DTA endotherm by using Kissinger's empirical relation (4).

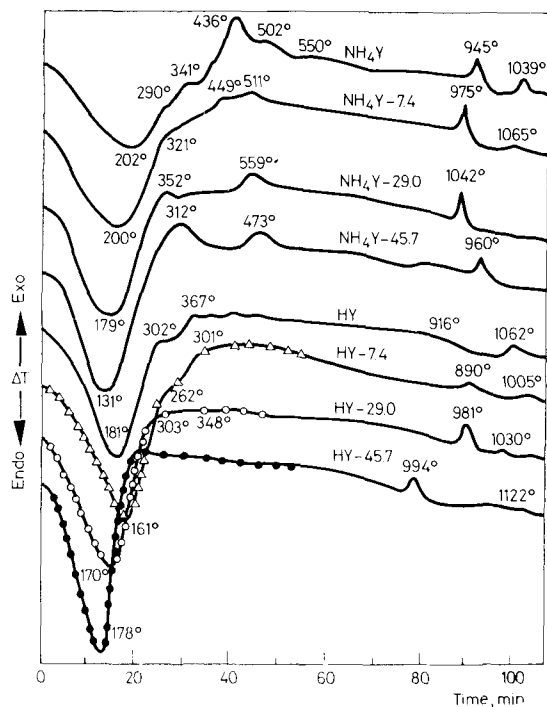


Fig. 2. Differential thermal curves of dealuminated and decationated zeolites

$$\log \left[ \frac{-\log(1-\alpha)}{T^2} \right] = \log \frac{AR}{Eb} \left[ 1 - \frac{2RT}{E} \right] - \frac{E}{2.303 RT} \quad (1)$$

$$\log \left( \frac{m}{T^2} \right) = A' - \frac{E}{2.303 RT} \quad (2)$$

$$\log \Delta T = C' = \frac{E_{DTA}}{2.303 RT} \quad (3)$$

$$n = 1.26 (S)^{1/2} \quad (4)$$

where  $m$  is the mass loss at time  $t$ ,  $\alpha$  is the relative mass loss,  $n$  the order of reaction,  $T$  the temperature,  $b$  the rate of heating of the sample,  $\Delta T$  the deviation of the DTA curve from the base line and  $S$  the shape index factor. The value of  $n$  was found to be nearly 1 and  $E$  decreased slightly (Table 1) with Al extraction from

NaY zeolite and also  $\text{NH}_4\text{Y}$  zeolite. This is consistent with the data reported for the steady decrease in  $T_{\text{max}}$  with dealumination and decationization and also with the decrease in the adsorption heats of water [12].

From the infrared spectra in the mid-frequency region ( $1300$  to  $250\text{ cm}^{-1}$ ), it was observed that almost all the bands shift to higher frequency with increase of dealumination. The most intense absorption band ( $950$  to  $1050\text{ cm}^{-1}$ ), related to

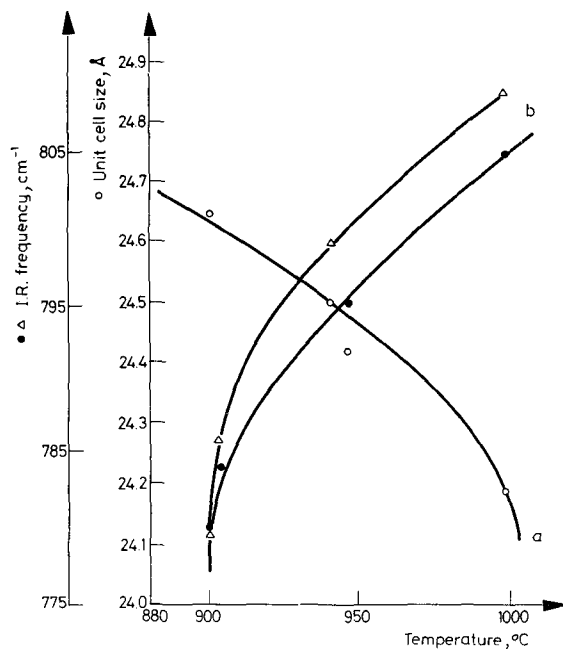


Fig. 3. Correlation of DTA structural collapse temperature with (a) unit cell size for NaY- $\alpha$   $\circ$  and (b) IR frequency for NaY- $\alpha$   $\bullet$  and  $\text{NH}_4\text{Y-}\alpha$   $\Delta$

the asymmetric stretching vibration of the T-O band (T = Si or Al), is shifted to higher frequency, as it is sensitive to the Si/Al ratio, as reported earlier for Linde 4A zeolite [21].

X-ray diffraction studies revealed that dealumination causes considerable lattice contraction. A lattice contraction of 1.01% occurred on removal of nearly 44% of the tetrahedral aluminum from normal hydrogen zeolite. On the other hand, for a similar quantity of Al extraction, the  $a_0$  value of dealuminated NaY is nearly 1.14% lower. The results obtained are in good agreement with the data of related studies on stabilized zeolites [15, 22, 23].

From the general survey, the thermal properties of modified zeolites have been related to structural modifying characteristics, such as IR frequency and unit cell dimensions (Fig. 3A and B). Such a correlation helps in predicting the changes which occur on dealumination/decationization or ion exchange. A decrease in

aluminium content leads to a decrease in some of the aluminosilicate bond lengths and an increase in the force constant, with resulting higher [24] IR vibrational frequencies.

### Conclusion

The suppositions involved in the method of calculation described above are true under the conditions of constancy of weight and rate of heating of reference samples and sample to be tested. The information acquired from the thermal curves in relation to IR and X-ray provides a useful background in studying various aspects of zeolites, it being concluded that the thermal stability of NaY and NH<sub>4</sub>Y zeolites increases with controlled dealumination of the framework structure.

\*

Thanks are due to Mr. C. V. Kavedia and Miss M. S. Agashe for assistance in thermal and IR spectroscopic analyses.

### References

1. G. T. KERR, *J. Phys. Chem.*, 72 (1968) 2954.
2. K. V. TOPCHIEVA and HUO SHIH T'HUANG, Contemporary problems in physical chemistry (in Russian), Vol. 8, Izd. Mosk. Un-ta (1975).
3. J. A. RABO, Actes du Deuxieme Congress Intern. de Catalyse, (1960) 2055.
4. G. T. KERR, *J. Catalysis*, 15 (1969) 200.
5. W. J. AMBS and W. J. FLANK, *J. Catalysis*, 14 (1969) 118.
6. G. T. KERR, *J. Phys. Chem.*, 73 (1969) 2780.
7. G. T. KERR, *J. Phys. Chem.*, 71 (1967) 4155.
8. P. JACOBS and J. B. UTTERHOEVEN, *J. Catalysis*, 22 (1971) 193.
9. F. PAULIK, J. PAULIK and L. ERDEY, *Talanta*, 13 (1966) 1405.
10. D. W. BRECK, *Zeolite Molecular Sieves, Structure, Chemistry and Use*, Pub. Wiley-Interscience, New York 1974.
11. I. V. MISHIN, G. A. PILOYAN, A. L. KLYACHKO-GURVICH and A. M. RUBINSSTEIN, *Bull. Akad. Sci. USSR.*, 22 (1973) 1298.
12. R. M. BARRER and E. V. MURPHY, *J. Chem. Soc., A* (1970) 2505.
13. A. P. BOLTON and M. A. LANEWALA, *J. Catalysis*, 18 (1970) 154.
14. P. CHU, *J. Catalysis*, 43 (1976) 346.
15. J. V. SMITH, *Molecular Sieve Zeolites-I*, *Advan. Chem. Ser.*, 101 (1971) 171.
16. P. D. HOPKINS, *J. Catalysis*, 12 (1968) 325.
17. W. J. AMBS and W. H. FLANK, *J. Catalysis*, 14 (1969) 118.
18. P. JACOBS and J. B. UTTERHOEVEN, *J. Catalysis*, 22 (1971) 193.
19. A. W. COATS and J. P. REDFERN, *Nature*, 68 (1964) 201.
20. G. O. PILOYAN and O. S. NOVIKOVA, *Inorganic Materials*; 2 (1966) 1109.
21. O. LAHODNY-ŠARC and J. L. WHITE, *J. Phys. Chem.*, 75 (1971) 2408.
22. C. V. MCDANIEL and P. K. MAHER, *Molecular Sieves, Society of Chemical Industry, London*, (1968) 186.
23. E. DEMPSY, G. H. KÜHL and D. H. OLSON, *J. Phys. Chem.*, 73 (1969) 387.
24. E. M. FLANIGEN and H. KHATAMI, *Molecular Sieve Zeolites-I. Advan. Chem. Ser.*, 101 (1971) 201.

RÉSUMÉ — La modification de la structure de squelette et la stabilité thermique des zéolites sous formes sodium et ammonium, ont été suivies à l'aide d'un dérivatographe. On a effectué des examens analogues par des méthodes indépendantes comme le sont l'IR et les rayons X. La comparaison a montré un bon accord entre les résultats. La «désalumination» contrôlée du zéolite Y augmente sa stabilité thermique.

ZUSAMMENFASSUNG — Der Derivatograph wurde zur Verfolgung der Änderungen der Skelettstruktur und Thermostabilität von Zeoliten in der Natrium- und Ammoniumform eingesetzt. Analoge Untersuchungen wurden durch unabhängige Methoden, wie IR und Röntgen, durchgeführt. Der Vergleich zeigte eine gute Übereinstimmung der Ergebnisse. Die gesteuerte Dealuminierung der Zeolite Y erhöhte ihre Thermostabilität.

Резюме — Был использован дериватограф для изучения изменения скелетной структуры и термической стабильности цеолитов в натриевой и аммониевой формах. Аналогичные исследования были проведены другими независимыми методами, такими как ИК спектроскопия и дифракция рентгеновых лучей. Полученные результаты показали хорошее совпадение друг с другом. Контролируемое деалюминирование цеолита у увеличивает его термическую стабильность.